Drying of Human Blood Drops

Houssine Benabdelhalim, David Brutin

CHAPTER 14

Drying of human blood drops

H. BENABDELHALIM[a]* and D. BRUTIN[a]*

[a] Aix Marseille Univ, CNRS, IUSTI, Marseille, France

*Corresponding contributors. E-mail: houssine.benabdelhalim@gmial.com ; david.brutin@univ-amu.fr

Abstract

The study of blood drop drying has attracted the attention of several research groups for two main reasons: (1) for biomedical purposes as a rapid and cheaper disease detector, and (2) for forensic applications for the interpretation of bloodstain at crime scenes. Also, it presents an interdisciplinary and challenging research subject. However, the mechanisms related to the formation of patterns at the end of the drying process are not fully understood, so this topic still represents an active branch of research that requires further efforts. When a drop of blood is deposited on a non-porous substrate in an unsaturated medium, it spreads and at the same time evaporates. The spreading is described by two regimes, a first regime controlled by the viscous-capillary balance and a second one controlled by the viscous-evaporation balance. The drop spreads until it reaches equilibrium, subsequently it keeps evaporating. The drying process is described by five distinct stages, and the final pattern is divided into three regions: the periphery, the corona, and the central region. The corona region results from the existence of a capillary flow inside the drop that transports the components to the edge of the drop (coffee ring effect). During the drying process, cracks form on the central region and the corona, this is explained in the literature by the competition between evaporation in the gel phase and adhesion to the substrate. These mechanisms (from spreading to final pattern formation) are influenced by the blood composition, the drop size, the substrate nature (wettability and contact angle), the relative humidity, and the temperature. In this chapter, we highlight the significant advances in the drying of human whole blood drops and the influence of these parameters.

4.1 Introduction

The drying of blood drops on a solid substrate leads to the formation of complex patterns, that can provide valuable information for two disciplines: forensic[1-4] and biomedical[5-8]. For forensic applications, bloodstains are one of the most encountered evidence at a crime scene after a bloody event[9]. Crime scene investigators examine this evidence and make conclusions such as how the blood was shed[2,10] and the time at which stains were created[1]. Chapter 15 provides more information for this purpose. For biomedical applications, the interpretation of dried human blood drops can be used as a clue to health status, as the morphology of the final drying pattern is highly dependent on the composition of the blood, and most diseases result in an alteration of this latter.

Several researchers have been interested in understanding the relationship between the final drying pattern of biological fluids (whole blood, plasma, and serum) and diseases to develop methods and tools that allow for fast and inexpensive diagnosis. Rapis[11] worked on the diagnosis of metastatic carcinoma by studying the drying of a human plasma film. He reported the existence of pronounced differences between the morphology of completely dried patterns of patients with the disease and those in good health. Yakhno et al.[12] investigated morphological differences in serum samples of patients with viral hepatitis B, chronic hepatitis B, and C. Buzoverya et al.[13] in their quantitative study investigated the possibility of associating the final drying pattern of plasma drops with different diseases, by determining structural inhomogeneities. Also, the work of Muravlyova et al.[14] on lung diseases. They used plasma samples collected from patients with interstitial lung fibrosis (ILF), patients with idiopathic interstitial pneumonia (IIP), and healthy people. They showed the existence of modifications between the patterns of the three studied groups, which was explained by the albumin existing in the plasma and the accumulation of extracellular nucleic acids.

The use of plasma and serum requires their separation from human whole blood, thus adding an extra step in sample preparation. The serum is plasma without the components that are involved in the coagulation cascade. On the other hand, the use of human whole blood drops avoids this extra step and the probable sample modifications related to this separation. Brutin et al.[5] are the first to describe fully the five stages of drying of human whole blood drops. Moreover, they reported the existence of a morphological difference between patterns obtained from healthy persons and those with diseases. In 2016, Bahmani et al.[8] conducted

a comparative study on the drying of whole blood drops for three patient groups: healthy, thalassemia, and neonatal jaundice. They showed that the morphology and more precisely the length of the cracks can be used as an indicator for these diseases.

The drying of blood drops is a complex phenomenon, which requires knowledge of biology, fluid mechanics, and heat and mass transfer. This is due to the composition of blood and its rheological behavior. Human blood is a colloidal suspension, composed mainly of plasma (interstitial fluid) and soft components (colloids) that interact with each other and can affect the physical mechanisms inside the drops. Where the plasma consists mainly of water. Human blood has a non-Newtonian behavior[15], and it represents thixotropic characteristics[15], i.e. its behavior evolves. When a blood drop is deposited on a substrate, it will spread until it reaches equilibrium. At the same time, the solvent (water) evaporates outside. The non-uniformity of the evaporation flow on the drop surface leads to the formation of a capillary flow inside the drop[16], which will transport the colloidal components towards the drop edge (coffee ring effect). The drying process is accompanied by a sol-gel phase change. In this gel phase, evaporation will take place through the pores created by the packing of the components. The competition between evaporation and adhesion to the substrate in this gel phase generates stresses, that will be released by the formation of cracks. These cracks characterize the final pattern of the dried blood drop [17-19].

The final pattern and mechanisms that lead to the formation of cracks in blood drops depend on parameters related to the health status of the person as the composition of blood. Also to external parameters: the size of the drop[5], the substrate on which the drop is created[20], the relative humidity[21], and the temperature[22]. Understanding the influence of these parameters on the drying of blood drops allows us to isolate or control their effect from changes related to pathological effects. In this chapter, we discuss the drying of blood drops from spreading to crack formation with a literature review. In addition, we summarize all parameters that influence spreading, evaporation, and crack formation.

4.2 Biological and physical properties of human blood

Blood is a fluid tissue, permanently conveyed in the circulatory system in a unidirectional flow imposed by

the cardiac pump. The whole human blood is composed of a cellular part (mainly red blood cells, white blood cells, and platelets), and a liquid part (plasma)[23]. The water represents 92 % of the total volume of plasma, the other part is proteins and different substances. Red blood cells (RBCs) or erythrocytes are the most abundant, they represent 97 % of the volume of the bio-colloidal matter. They have biconcave disc shape. Their volume percentage in the blood is given by a dimensionless quantity known as the hematocrit level (hct). This latter varies between 38 % and 50 % for a healthy person. Under pathological conditions, the hematocrit may fall as low as 20% and rise to about 70%. Where the rheology and the viscosity of the blood depend strongly on the RBCs. White blood cells (WBCs) or leukocytes, are cells of the immune system. Due to their low physiological number in the blood, they contribute little to the mechanical properties of the blood. Platelets or thrombocytes play a major role in primary hemostasis; they are involved in coagulation. And they are of little rheological importance because they are very small components that do not interact with each other under normal conditions. Outside the human body, blood naturally coagulates and forms clots. During this process, fibrinogens of the plasma will be consumed, and it becomes serum.

The whole human blood is a complex non-Newtonian fluid that can be considered as a colloidal suspension[15]. It is characterized by a shear-thinning behavior, where its dynamic viscosity decreases with the increase of the shear rate. At shear rates higher than 100 s^{-1}, blood behaves like a Newtonian fluid with a dynamic viscosity equal to 4 mPa.s at a temperature of 37 °C. The blood viscosity depends on the measurement method[15], temperature[15], and hematocrit level[15,24]. Harkness and Philips[15] reported a decrease of 3 % per 1 °C of the dynamic viscosity with the increase of the temperature. However, the increase in the hematocrit level causes an increase in the dynamic viscosity, which is greater at low shear rates. Although, the serum has a Newtonian behavior with a constant value of dynamic viscosity at any value of the shear rate, which is equal to 1.23 mPa.s under a temperature of 37 °C.

The surface tension of whole human blood and serum are described by a linear equation as a function of temperature in the range of 20 °C to 40 °C [25]:

For whole blood $\sigma = (-0.473 \times T + 70.105) \times 10^{-3}$ and for serum $\sigma = (-0.368 \times T + 66.072) \times 10^{-3}$.

Where σ, represent the surface tension on N/m, and T , represent the temperature on °C.

4.3 Drying of whole human blood drop

From a kinetic point of view, the drying study is the characterization of the variation of the mass and the rate of evaporation as a function of time. Also, to determine the sorption curves according to the surrounding conditions. From a dynamic and morphological point of view, it is the characterization of the different forces that interact during the whole process and the description of the visual aspect. However, the understanding of the drying of blood drops requires the consideration of both approaches. The drying process of blood drops is a complex phenomenon that exhibits coupled physical mechanisms, such as spreading, evaporation, Marangoni flow, wetting, coffee ring effect, gelation, and crack formation. It was shown that under the same experimental conditions, this process is reproducible, and the final pattern depends only on the composition of the blood[5].

When a blood drop is gently deposited on a non-porous substrate in an unsaturated medium, spreading and evaporation take place. The drop spreads to minimize its system energy and evaporates owing to the existence of a difference between the vapor concentration on the drop surface and the surrounding. Bouzeid and Brutin[21] studied the spreading dynamics of a drop of human blood on a clean glass substrate under a temperature of 25.5 ± 0.5 °C and relative humidity of 65 ± 2 %. Figure 14.1 shows the variation of the normalized radius of the drop as a function of time normalized by using the total evaporation time t_f. This latter is defined as the time on which there is no solvent losing anymore, hence no mass variation. This time is given by:

$$t_f = \frac{4RTm_0}{\pi \Delta P D_f D_{diff}} \tag{14.1}$$

Where D_{diff} the coefficient of diffusion (for blood drop drying at 25 °C, this coefficient is $2.19 \times 10^{-5}\ m^2/s$), T is the air temperature, R is the gas constant, m_0 is the initial drop mass, D_f is the final wetting diameter of the wetted area, and ΔP is the difference between the saturated pressure and the air pressure.

The authors distinguished two different spreading regimes, where the first regime is faster than the second Figure 14.1. They determined the driving forces and the nature of dissipation in each regime. By using dimensionless numbers, they compared the forces involved in the spreading of a blood drop. During both regimes, the Bond number was less than 1, therefore the drop shape is spherical cap, and the gravitational forces can be neglected. Where they showed that the spreading is controlled by the balance of capillary and

viscous forces in the first regime, and it is characterized by a power-law time evolution with exponent n = 0.65. While the second regime is described by the balance of driving forces generated by evaporation and viscous forces with a spreading exponent n = 0.18.

[Figure 14.1 near here]

The blood drop spreads until reaching a wetting radius and a wetting contact angle. At this time, the contact line is pinned to the substrate. In fact, for biological fluids, proteins anchor the contact line, as they will be absorbed by the substrate[26]. The drop volume at equilibrium is given as function of the radius R_f and contact angle θ_f, as follow:

$$V(R_f, \theta_f) = \frac{\pi R_f^3}{3} \frac{(1 - cos\theta_f)^2 (2 + cos\theta_f)}{(\sin^3 \theta_f)} \tag{14.2}$$

On the other hand, evaporation continues until the drop is completely dry. A blood drop evaporates with constant contact area. Brutin et al.[5] have divided the drying process of a blood drop into 5 distinct stages Figure 14.2. Where each stage is driven by specific mechanisms:

[Figure 14.2 near here]

(1) Stage 1, the evaporation of the solvent and the surface tension gradient induces a Marangoni flow, consequently, this flow moves the biocolloid components towards the contact line[16,27,37]. The accumulation of these components creates a red deposit at the edge of the drop. Also, a drying front forms as the solvent continues to evaporate.

(2) Stage 2, the drying process continues by the propagation of the drying line towards the center of the drop. The inner flow creates a difference in fluid composition, which results in the formation of a dark red torus.

(3) Stage 3, the Marangoni flow is no longer possible since the volume fraction of the solid components has increased, and now the drop has a flat central area. The torus dries quickly, and the central part becomes lighter red. At the end of this stage, most of the cell components are in the so-called corona zone Figure 14.3 and some RBCs are trapped in the central zone. A first crack appears around the drop between the corona and the central part of the drop.

(4) Stage 4, The drying of the corona area is completed, and circular drying patterns are observed

around the corona. The central area starts to dry completely and shows the formation of small cracks.

(5) Stage 5, During this stage, the large, wide plates of the corona move slightly. At the end of the drying process, the final pattern has a donut shape with a typical cross-sectional deposit.

Brutin et al.[5] realized several drying blood drops experiments under the same conditions, for each dried drop they obtained a final pattern with the same characteristics Figure 14.3: The central part of the drop, the large moving plates of the corona with wide white cracks, and the fin periphery. Whereas the central part of the drop and the fin periphery adhere to the glass plate due to the absence of RBCs, the corona is where the mobile deposits form and these do not adhere to the substrate. This is due to the presence of proteins in the RBCs (glycoproteins). The role of these proteins is to avoid wetting with the veins. The final drop pattern is highly dependent on the substrate wettability, drop size, relative humidity, and temperature. The influence of all these parameters is given in detail in the following sections.

[Figure 14.3 near here]

In the first stages of drying, the drop is in a liquid state. The drying is characterized by the evaporation rate. Where in hydrophilic situations, the evaporation rate of the solvent is higher near the contact line, which results in a radial internal flow[16,27,37]. This flow transports the bio-colloidal components towards the contact line, which will accumulate and reinforce the pinning of the contact line. This phenomenon is known as the "coffee stain effect". Sobac and Brutin[28] observed an increase in concentration at the contact line, which is important since the volume of fluid is locally small and decreases during evaporation. At a critical concentration value, the particles aggregate and form a gel[27,29]. Hence the formation of a gel front at the edge of the drop, although the central part is still liquid. The gel front will propagate as the concentration increases due to the evaporation of the solvent. The first cracks nucleate on the gelled region near the contact line. Afterward, these cracks, which are evenly spaced radially, propagate inward as they are stretched by the movement of the front. After complete gelation of the drop, some solvent is trapped inside the formed porous matrix. Drying continues by diffusion of solvent molecules through the pores, with a decrease in the rate of evaporation, so radial cracks continue to propagate. At the end of drying, disordered cracks are formed in the central part of the drop.

During the loss of the solvent in the gel phase, important mechanical stress is formed due to the high capillary pressure in the tightly packed colloidal components. This stress leads to the appearance of two types of instabilities upon its release[30], either the formation of cracking or buckling instabilities on the drop surface. The existence or not of one of these instabilities depends on the surface wettability, the composition of the drop, and the surrounding conditions. In this chapter, we will only focus on the formation of cracks since it is the most common instability encountered in the drying of the blood drop on clean glass. The dynamics of their development were studied by several researchers, in the case of different fluids and for different applications, ranging from mud[31] to nano-fluid drops[32].

The mechanisms of crack formation in human blood drops have been well described by Sobac and Brutin[28]. They investigate the dynamics of rupture, average crack size, and delamination. Also, they showed that the spacing of the first crack matches perfectly with that predicted by Allain and Limat[33].

[Figure 14.4 near here]

When gelation takes place, the trapped solvent starts to evaporate through the pores. This effect results in an intensification of the aggregation of the particles, hence consolidation of the gel. In this stage, the system is described by two interfaces Figure 14.4, a liquid-vapor interface where there is the evaporation of the solvent, and a gel-substrate interface. In the first interface, menisci form and are responsible for capillary pressure in the liquid phase $P_{cap} = -(2\gamma_{s,a}\cos\theta)/r_p$. Where $\gamma_{s,a}$ is the solvent-air surface tension, θ is the liquid-solid contact angle, and r_p is the pore radius. During evaporation, the curvature of the menisci increases, which will generate a depression in the solvent. The pressure gradient leads to a migration of the solvent towards the surface and a progressive shrinking of the gel in response to the compressive force. This shrinkage is limited by the adhesion of the drop to the substrate. The competition between evaporation and adhesion leads to the development of mechanical stress, which will increase during drying and is released by the formation of cracks[17,18]. The ability of the gel to fracture depends on the significant existence of a pressure gradient in the pores[30].

Choi et al.[7] proposed a theoretical model to understand and predict crack density in a dry drop of blood. Their model is validated by experiments on colloidal suspensions and whole blood. Also, this model takes into account the effect of relative humidity and viscosity. The density of cracks is given by:

$$f = \frac{1}{\lambda} \sim \frac{\mu r (1 - RH)^{\frac{3}{4}}}{\eta^{\frac{1}{4}} \sigma^{\frac{3}{4}} K} \quad (14.3)$$

With, λ the distance between cracks, μ the solvent viscosity, r the characteristic size, RH the relative humidity, η the dispersion viscosity, K the permeability of the porous medium.

4.3.1 Effect of the blood drop size

Brutin et al.[5] studied the effect of drop size on crack formation in the so-called corona region, on a clean glass substrate, under a relative humidity of 47% and temperature of 22 °C, Figure 14.5. They reported that the number of cracks increases with the increase of the blood drop diameter, which is observed only from a critical diameter equal to 4.5 mm. Drops with larger diameters clearly show large, axisymmetric, and periodic cracks around the corona. However, for drops with diameters below this critical value, they did not observe axisymmetric cracks in the corona, Figure 14.5. In the previous section, we mention that the formation of the cracks is due to the developed stress. This latter results from the competition between evaporation and adhesion. This stress is lower for small drops than the one existing in drops with a diameter greater than 4.2 mm.

[Figure 14.5 near here]

4.3.4 Effect of substrate nature

The wettability, porosity, and thermal characteristics of a substrate have an important contribution to the formation of the final drop pattern. They mainly affect the coffee ring effect, transport of solid components, stress in the drop, and cracks formation. The wetting of a drop on a non-porous substrate is described by the apparent contact angle measured at equilibrium, i.e., when the spreading stops. This contact angle describes the geometry and drying process of the drop[34]. Recently, Hertaeg et al.[35] have developed a model to predict the apparition of the coffee ring phenomenon. They showed that at a given volume fraction, there is a critical value of contact angle below which the coffee ring effect is observed. Also, at a given volume fraction, and a contact angle below a threshold value, this effect is observed. That was explained by the fact that the contact angle influences the dominance of the viscous effects on the surface tension.

Chen et al.[34] showed that the initial contact angle influences the final blood drop pattern. They used a glass

substrate, which can control the contact angle. Three drops with different contact angles: 20 °, 35 °, and 50 ° were created. Figure 14.6 shows the morphological details obtained as a function of contact angle:

[Figure 14.6 near here]

(1) The width of the peripheral region decreases with increasing contact angle since the local thickness in this region increases with the contact angle. They explained this by using the Griffith theory[36], to determine the critical crack size. (Figure 14.6.a-c small red box)

(2) In the corona region Figure 14.6.a-c, they found that there is no change in crack characteristics, morphology, and spacing. They created drops of the same volume 12 um. These drops lose the same amount of solvent during the drying process; hence the same amount of energy will be released for crack formation. As a result, the same morphology for the three contact angles.

(3) The central region morphology depends on the initial contact angle, since the contact angle has a direct influence on the internal flow of the drop, hence on the transport and distribution of RBCs. Figure 14.6.d-f clearly shows the effect of the contact angle on this region. The latter increases with increasing contact angle; however, the number of plates and random cracks decreases with increasing contact angle.

The wetting of the substrate has a relevant influence on the drying of a blood drop, unlike the thermal diffusivity of the substrate[20]. Brutin et al.[20] investigated the contribution of these two parameters on the drying dynamics and the morphology of the final pattern. They performed experiments on three different substrates Figure 14.7: A glass substrate with an initial contact angle of 20.5 °, an initial thickness of 410 µm, and a final thickness of 50 µm. A gold substrate with a contact angle of 91.1 ° and an initial thickness of 1.53 mm. An aluminium substrate with a contact angle of 95.7 ° and an initial thickness of 1.66 mm.

[Figure 14.7 near here]

They showed that the evaporation dynamics and drying time on the three substrates is almost the same despite the fact that aluminium has a high thermal diffusivity. There is a first regime of linear decrease when the drop is mainly liquid, and a second regime with a sharp decrease associated with the end of gelation. The dynamics of evaporation is the same because the limiting factor is the diffusion of the solvent vapor outside.

The drying of a drop on a glass substrate is already considered in the previous sections. For the other two substrates with a contact angle of about 90 °, the morphology is completely different. During the drying process, a glassy skin is formed in the drop/liquid interface, afterwards this plastic shell will deform and leads to the final pattern as shown in Figure 14.7.b-c. They associated this phenomenon with the evaporation dynamics. In the case of a wetting drop with a contact angle less than 40°, the evaporation rate high along the periphery and decreases across the interface[37]. Although in the case of a non-wetting drop, about 90 °, the evaporation rate is mostly constant across the interface[37]. In the latter case, RBCs will not be transported to the edge of the drop, hence no coffee ring effect. Also, the drops at the end of the drying dewet and retract from the metal substrate and develop a hole in the center of the drop Figure 14.7.b-c. Pauchard et allain[18] observed the same pattern for polymer drops, which was explained by the "buckling" phenomenon.

4.3.2 Effect of the relative humidity

The evaporation rate is a function of the relative humidity, it can be almost zero in saturated environments ($RH = 100\%$), as it can be maximum at low relative humidities. Therefore, its value decreases with increasing humidity. The evaporation rate describes the speed at which a drop of a volatile fluid evaporates. Bouzeid and Brutin[21] investigated the effect of relative humidity (RH) on the spreading of blood drops, under a temperature of 25.5 ± 0.5 °C and a relative humidity rank ranging from 8% to 90%. They showed that at low evaporation rates (high RH), the spreading is quick in contrast to high evaporation rates (low RH) Figure 14.8. Hence the equilibrium drop area increases with increasing RH. This is because solvent loss is lower at high RH, then more solvent will spread out. Also, the rate of contact line advancement decreases with increasing RH. Bouzeid and Brutin[38] constate a linear variation of the contact angle as function of humidity, which is given by the following equation:

$$\theta_{RH} = 21(1 - RH) \tag{14.4}$$

That was obtained by fitting the experimental results. The substitution of the equation (14.4) into equation (14.2) provides the radius variation with RH:

$$R_{RH} = \left(\frac{3V}{\pi}\frac{\sin^3\theta_{RH}}{(2+\cos\theta_{RH})(1-\cos\theta_{RH})^2}\right)^{\frac{1}{3}} \tag{14.5}$$

Hu and Larson[37] derived a simple analytical expression to describe the evaporation rate of droplet, which is valid for the case with a constant area drying mode and contact angle less then 90 °. This latter was described by Bouzeid and Brutin[38] for blood droplet and as function of RH as flow:

$$J_{blood} = \pi R_{RH} D_{diff} C_v (1 - RH) f_{RH} \tag{14.6}$$

where $C_v(1 - RH)$ is the vapor concentration difference between the saturated vapor at the apex and the vapor concentration in the far-field from the drop and f_{RH} is a function that depends on the contact angle and the relative humidity given by:

$$f_{RH} = (3.59 \times 10^{-2})RH^2 - (7.18 \times 10^{-2})RH + 1{,}33 \tag{14.7}$$

[Figure 14.8 near here]

In another study, Bouzeid and Brutin[38] investigated the effect of relative humidity on the final dried drop pattern. In a range of relative humidity from 13.5 % to 78.0 %, on a clean glass substrate. They showed that the relative humidity has a strong influence on the contact angle, the final pattern, and the end of the drying process. The contact angle decreases with RH, which will influence the final pattern. Figure 14.9 shows the different final patterns obtained at the end of the drying process as a function of RH. The surface of the mobile plates in the corona depends on the relative humidity. By the change in evaporation rate, the mechanical properties of the gel are changed such as the adhesion to the substrate. They found a decrease in adhesion energy at RH ranging from 13.5% to 50.0%, from which the surface area of the plates becomes progressively large. For patterns obtained at RHs above 50%, the mobile plates are smaller with significant adhesion energy. In contrast, the width of the drop edge increases continuously as a function of RH, the yellow lines in Figure 14.9. This thin edge is due to the absence of RBCs caused by the propagation of the gel front.

[Figure 14.9 near here]

Using model (14.3), Choi et al.[7] predicted crack density as a function of relative humidity in whole blood drops and colloidal suspensions. They reported a decrease in crack density as a function of relative humidity. Also, their model is in agreement with the experimental results, presented by the solid line

Figure 14.10.

[Figure 14.10 near here]

4.3.3 Effect of the temperature and the concentration

In this section, we will highlight the recent work of Pal et al.[22] on the effect of temperature and concentration on the drying morphology of blood drops. In this regard, they created drops of 1 ul volume with different concentrations ranging from 12.5 % up to 100 %, on a substrate with a controlled temperature of 25 °C to 45 °C, under 50 % relative humidity. Figure 14.11 shows the final patterns obtained after the total drying.

[Figure 14.11 near here]

At 25 °C, there are all the regions seen previously in the work of Brutin et al.[5], the central region, and the so-called corona region. At 45 °C, the central region is absent at concentrations higher than 62 %. They reported that cracks morphology does not represent a significant difference depending on the three temperatures studied. The temperature of the substrate will reduce drying time, and it will intensify the Marangoni flow inside the drop, hence increasing the internal flow velocity. However, the width of the corona increases with the concentration and the width of the central region decrease. Recently, Parthasarathy et al.[39] observed the same behavior as a function of concentration and particle size. They attribute this suppression of the corona "coffee ring effect" to components aggregation. Pal et al.[22] showed the existence of a difference in the drying process as a function of concentration, at a concentration of 100 %, the cracks propagate radially from the center to the edge, in contrast to a concentration of 12.5 %, in which the cracks propagate from the edge to the center. The central region and corona have different thicknesses for concentrations of 50 to 12.5 %, in contrast to concentrations of 100 % to 62 %, in the latter the difference is not too visible. Also, the number of cracks increases, and the spacing between cracks becomes thin with decreasing concentration.

4.4 Conclusion

The final pattern of a completely dried blood drop can be used as a biological marker for certain diseases, since it represents a fast procedure and does not require large quantities of human blood. For this purpose, it is necessary to clearly distinguish between the effect of blood composition and other external parameters on

the dried pattern. The mechanisms that lead to the formation of the final pattern are complex. In order to understand them, several important works have been done so far, in which the influence of external parameters is taken into account. However, our knowledge about the link between the morphology of the final patterns and a given disease is not yet clear. Therefore, further studies on cellular and molecular biophysical interactions are needed before moving on to medical applications.

References*

1. Smith, F. R.; Nicloux, C.; Brutin, D. A New Forensic Tool to Date Human Blood Pools. *Scientific Reports* 2020, **10** (1), 1–12.

2. Laan, N.; de Bruin, K. G.; Bartolo, D.; Josserand, C.; Bonn, D. Maximum Diameter of Impacting Liquid Droplets. *Phys. Rev. Applied* 2014, **2** (4), 044018.

3. Laan, N.; Smith, F.; Nicloux, C.; Brutin, D. Morphology of Drying Blood Pools. *Forensic Science International* 2016, **267**, 104–109.

4. Attinger, D.; Moore, C.; Donaldson, A.; Jafari, A.; Stone, H. A. Fluid Dynamics Topics in Bloodstain Pattern Analysis: Comparative Review and Research Opportunities. *Forensic Science International* 2013, **231** (1–3), 375–396.

5. Brutin, D.; Sobac, B.; Loquet, B.; Sampol, J. Pattern Formation in Drying Drops of Blood. *J. Fluid Mech.* 2011, **667**, 85–95.

6. Chen, R.; Zhang, L.; Zang, D.; Shen, W. Blood Drop Patterns: Formation and Applications. *Advances in Colloid and Interface Science* 2016, **231**, 1–14.

7. Choi, J.; Kim, W.; Kim, H.-Y. Crack Density in Bloodstains. *Soft Matter* 2020, **16** (24), 5571–5576.

8. Bahmani, L.; Neysari, M.; Maleki, M. The Study of Drying and Pattern Formation of Whole Human Blood Drops and the Effect of Thalassaemia and Neonatal Jaundice on the Patterns. *Colloids and Surfaces A: Physicochemical and Engineering Aspects* 2017, **513**, 66–75.

9. James, S. H.; Kish, P. E.; Sutton, T. P. *Principles of Bloodstain Pattern Analysis: Theory and Practice*; Practical aspects of criminal & forensic investigation; CRC: Boca Raton, Fla, 2005.

10. Boos, K.; Orr, A.; Illes, M.; Stotesbury, T. Characterizing Drip Patterns in Bloodstain Pattern Analysis: An Investigation of the Influence of Droplet Impact Velocity and Number of Droplets on Static Pattern Features. *Forensic Science International* 2019, **301**, 55–66.

Lowe, G. D. O. *Clinical Blood Rheology. Volume I Volume I*; 2019.

11. Rapis, E. A Change in the Physical State of a Nonequilibrium Blood Plasma Protein Film in Patients with Carcinoma. *Tech. Phys.* 2002, **47** (4), 510–512.

12. Yakhno, T. A.; Sedova, O. A.; Sanin, A. G.; Pelyushenko, A. S. On the Existence of Regular Structures in Liquid Human Blood Serum (Plasma) and Phase Transitions in the Course of Its Drying. *Tech. Phys.* 2003, **48** (4), 399–403.

13. Buzoverya, M. E.; Shcherbak, Yu. P.; Shishpor, I. V. Quantitative Estimation of the Microstructural Inhomogeneity of Biological Fluid Facies. *Tech. Phys.* 2014, **59** (10), 1550–1555.

14. Muravlyova, L.; Molotov-Luchanskiy, V. B.; Bakirova, R. Y.; Zakharova, Y. E.; Klyuyev, D. A.; Bakenova, P. A.; Demidchik, L. A.; Suleimenova, S. B. Structure-Forming Properties of Blood Plasma of Patients with Interstitial Lung Diseases. *World Journal of Medical Sciences* 2014, **10** (4), 478–483.

15. Lowe, G. D. O. *Clinical Blood Rheology. Volume I Volume I*; 2019.

16. Deegan, R. D.; Bakajin, O.; Dupont, T. F.; Huber, G.; Nagel, S. R.; Witten, T. A. Capillary Flow as the Cause of Ring Stains from Dried Liquid Drops. *Nature* 1997, **389** (6653), 827–829.

17. Lei, H.; Francis, L. F.; Gerberich, W. W.; Scriven, L. E. Stress Development in Drying Coatings after Solidification. *AIChE journal* 2002, **48** (3), 437–451.

18. Pauchard, L.; Allain, C. Stable and Unstable Surface Evolution during the Drying of a Polymer Solution Drop. *Physical Review E* 2003, **68** (5), 052801.

19. Lazarus, V.; Pauchard, L. From Craquelures to Spiral Crack Patterns: Influence of Layer Thickness on the Crack Patterns Induced by Desiccation. *Soft Matter* 2011, **7** (6), 2552–2559.

20. Brutin, D.; Sobac, B.; Nicloux, C. Influence of Substrate Nature on the Evaporation of a Sessile Drop of Blood. *Journal of heat transfer* 2012, **134** (6).

21. Bouzeid, W.; Brutin, D. Effect of Relative Humidity on the Spreading Dynamics of Sessile Drops of Blood. *Colloids and Surfaces A: Physicochemical and Engineering Aspects* 2014, **456**, 273–285.

22. Pal, A.; Gope, A.; Iannacchione, G. Temperature and Concentration Dependence of Human Whole Blood and Protein Drying Droplets. *Biomolecules* 2021, **11** (2), 231.

23. Thiriet, M. *Biology and Mechanics of Blood Flows*; CRM series in mathematical physics; Springer: New York ; London, 2008.

24. Chao, T. C.; Trybala, A.; Starov, V.; Das, D. B. Influence of Haematocrit Level on the Kinetics of Blood Spreading on Thin Porous Medium during Dried Blood Spot Sampling. *Colloids and Surfaces A: Physicochemical and Engineering Aspects* 2014, **451**, 38–47.

25. Rosina, J.; Kvasnak, E.; Suta, D.; Kolarova, H.; Malek, J.; Krajci, L. Temperature Dependence of Blood Surface Tension. *Physiological Research* 2007, **56** (1), S93.

26. Tarasevich, Y. Y.; Pravoslavnova, D. M. Segregation in Desiccated Sessile Drops of Biological Fluids. *The European Physical Journal E* 2007, **22** (4), 311–314.

27. Popov, Y. O. Evaporative Deposition Patterns: Spatial Dimensions of the Deposit. *Physical Review E* 2005, **71** (3), 036313.

28. Sobac, B.; Brutin, D. Desiccation of a Sessile Drop of Blood: Cracks, Folds Formation and Delamination. *Colloids and Surfaces A: Physicochemical and Engineering Aspects* 2014, **448**, 34–44.

29. Bodiguel, H.; Doumenc, F.; Guerrier, B. Stick− Slip Patterning at Low Capillary Numbers for an Evaporating Colloidal Suspension. *Langmuir* 2010, **26** (13), 10758–10763.

30. Giorgiutti-Dauphiné, F.; Pauchard, L. Drying Drops. *The European Physical Journal E* 2018, **41** (3), 1–15.

31. Goehring, L.; Nakahara, A.; Dutta, T.; Kitsunezaki, S.; Tarafdar, S. *Desiccation Cracks and Their Patterns: Formation and Modelling in Science and Nature*; John Wiley & Sons, 2015.

32. Carle, F.; Brutin, D. How Surface Functional Groups Influence Fracturation in Nanofluid Droplet Dry-Outs. *Langmuir* 2013, **29** (32), 9962–9966.

33. Allain, C.; Limat, L. Regular Patterns of Cracks Formed by Directional Drying of a Collodial Suspension. *Physical review letters* 1995, **74** (15), 2981.

34. Chen, R.; Zhang, L.; Shen, W. Controlling the Contact Angle of Biological Sessile Drops for Study of Their Desiccated Cracking Patterns. *Journal of Materials Chemistry B* 2018, **6** (37), 5867–5875.

35. Hertaeg, M. J.; Rees-Zimmerman, C.; Tabor, R. F.; Routh, A. F.; Garnier, G. Predicting Coffee Ring Formation upon Drying in Droplets of Particle Suspensions. *Journal of colloid and interface science* 2021, **591**, 52–57.

36. Xu, Y.; German, G. K.; Mertz, A. F.; Dufresne, E. R. Imaging Stress and Strain in the Fracture of Drying Colloidal Films. *Soft Matter* 2013, **9** (14), 3735–3740.

37. Hu, H.; Larson, R. G. Evaporation of a Sessile Droplet on a Substrate. *The Journal of Physical Chemistry B* 2002, **106** (6), 1334–1344.

38. Bouzeid, W.; Brutin, D. Influence of Relative Humidity on Spreading, Pattern Formation and Adhesion of a Drying Drop of Whole Blood. *Colloids and Surfaces A: Physicochemical and Engineering Aspects* 2013, **430**, 1–7.

39. Parthasarathy, D.; Thampi, S. P.; Ravindran, P.; Basavaraj, M. G. Further Insights into Patterns from Drying Particle Laden Sessile Drops. *Langmuir* 2021.

Figure Captions

Figure 14.1 Evolution of the dimensionless radius, $(r(t) - R0)/(Rf - R0)$, as a function of dimensionless time, t/t_F, at $RH = 65\%$. The inset graph is a plot in a log-log representation[21]. Copyright 2014 Elsevier.

Figure 14.2 Time-lapse of a drying blood drop with 5.9 mm of diameter on microscope glass substrate at temperature of 22 °C, showing the five distinct stages[5]. Copyright 2011 Cambridge University Press.

Figure 14.3 Closer view of pattern of a dried blood drop with 5.9 mm of diameter on microscope glass substrate at 22 °C, showing the three different regions[5]. Copyright 2011 Cambridge University Press.

Figure 14.4 Schematic representation of the formation of a porous matrix during the drying process. A close packed array of particles saturated by solvent is formed. The system is bounded by two interfaces: the solid-gel interface and the gel–air interface. A curvature of the solvent–air menisci occurs at the evaporation surface and increases during solvent loss. The competition between the mechanisms occurring at the two interfaces, i.e., adhesion and evaporation, leads to crack formation. r and r' denote the curvature of the menisci before and after shrinkage, respectively[19]. Copyright 2011 Royal society of chemistry.

Figure 14.5 Cracks number in the corona as a function of drop diameter. All drops are created with the same blood on a microscope glass substrate under a temperature of 22 °C and relative humidity of 47 %[5]. Copyright 2011 Cambridge University Press.

Figure 14.6 Corona (left) and centrale region (right) morphology as a function of initial contact angles: (a,d) $\theta = 20°$, (b,e) $\theta = 35°$, and (c,f) $\theta = 50°$. The small red box represents the peripheral region in (a–c). L represent the length of large plaques[34]. Copyright 2018 Royal society of chemistry.

Figure 14.7 Morphologies of dried blood drops formed on different substrates: (a) glass; (b) gold; (c) aluminum[20]. Copyright 2012 American Society of Mechanical Engineers.

Figure 14.8 Schematic representation of spreading drops for the case of: (a) RH = 10 % and (b) RH = 80 %. Initially, the blood drop has a spherical shape, and at equilibrium the drop has the shape of a spherical cap. The arrows indicate the velocity and evaporative flux of water vapour from the drop surface to the surroundings in the vicinity of the triple line. The dashed square marks the area close to the triple line, where the drop geometry can be approximated by a wedge[21]. Copyright 2014 Elsevier.

Figure 14.9 Dried pattern morphology as a function of relative humidity (RH varying between 13.5 % and 78.0 %). Area between dashes in yellow represents the fine periphery corona[38]. Copyright 2013 Elsevier.

Figure 14.10 Crack density measurement and visualization as a function of relative humidity. Measurement was carried out by using the equation 14.3 (denoted by Eq. (1) on the graph). The visual results of blood drop were compared with mono and binary size colloid dispersion[7]. Copyright 2020 Royal society of chemistry.

Figure 14.11 Final pattern of whole human blood drops at different initial concentrations ($\emptyset_b$) ranging from 100 to 12.5% (v/v), dried under three different substrate temperature of 45 °C, 35 °C, and 25 ◦C. The scale bar of length 0.2 mm is represented by the white rectangle in the top-right panel[22]. Copyright 2021 MDPI.

Figures

Figure 14.1

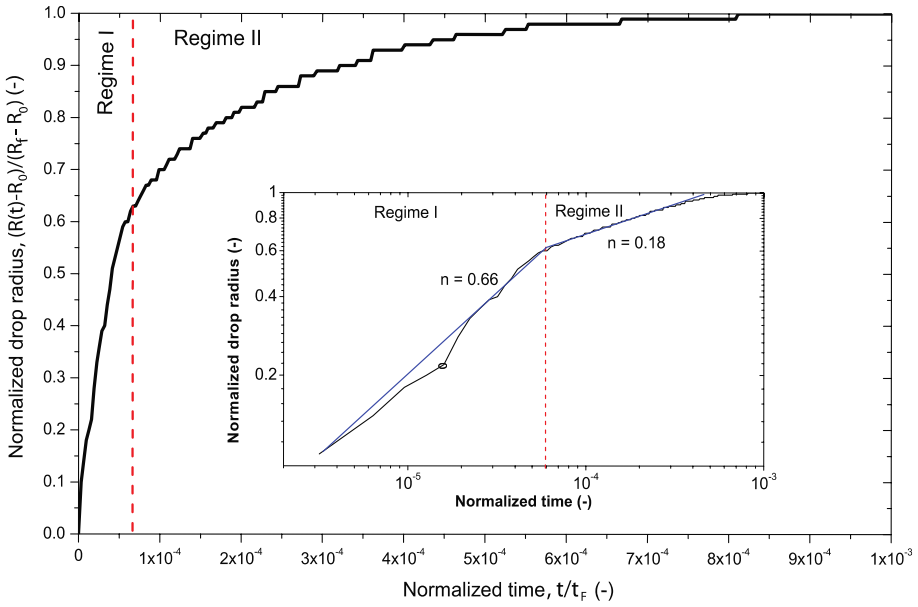

Figure 14.2

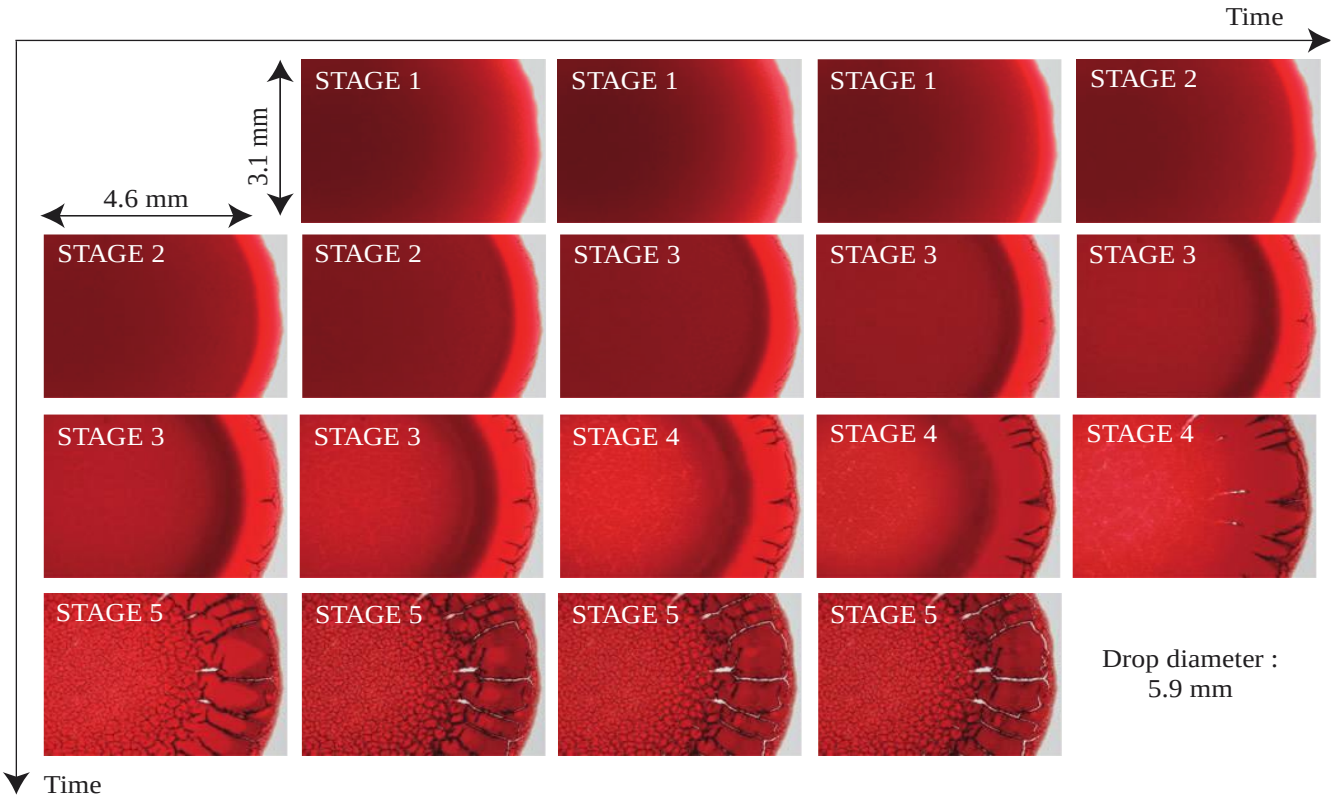

Figure 14.3

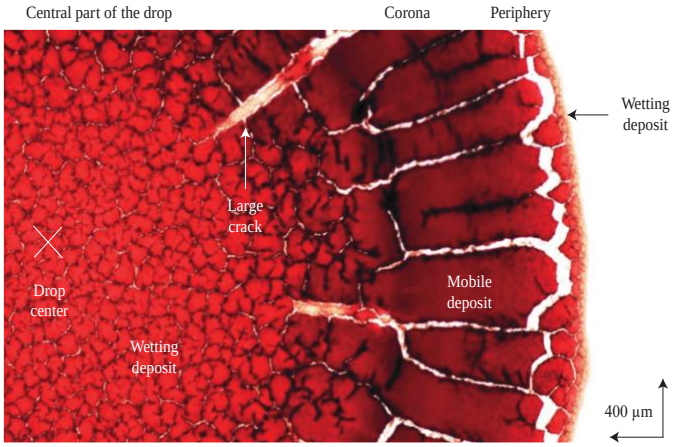

Figure 14.4

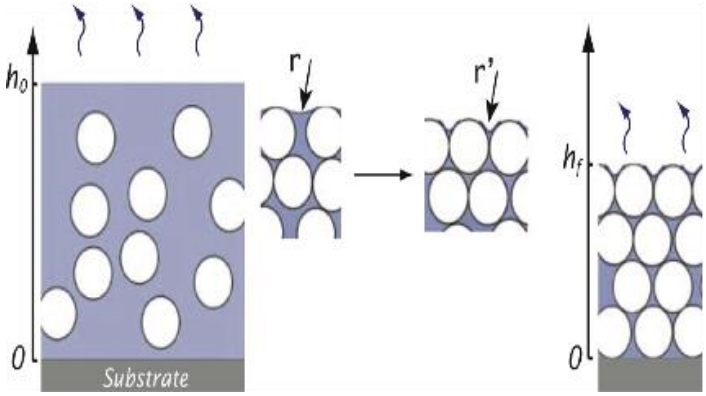

Figure 14.5

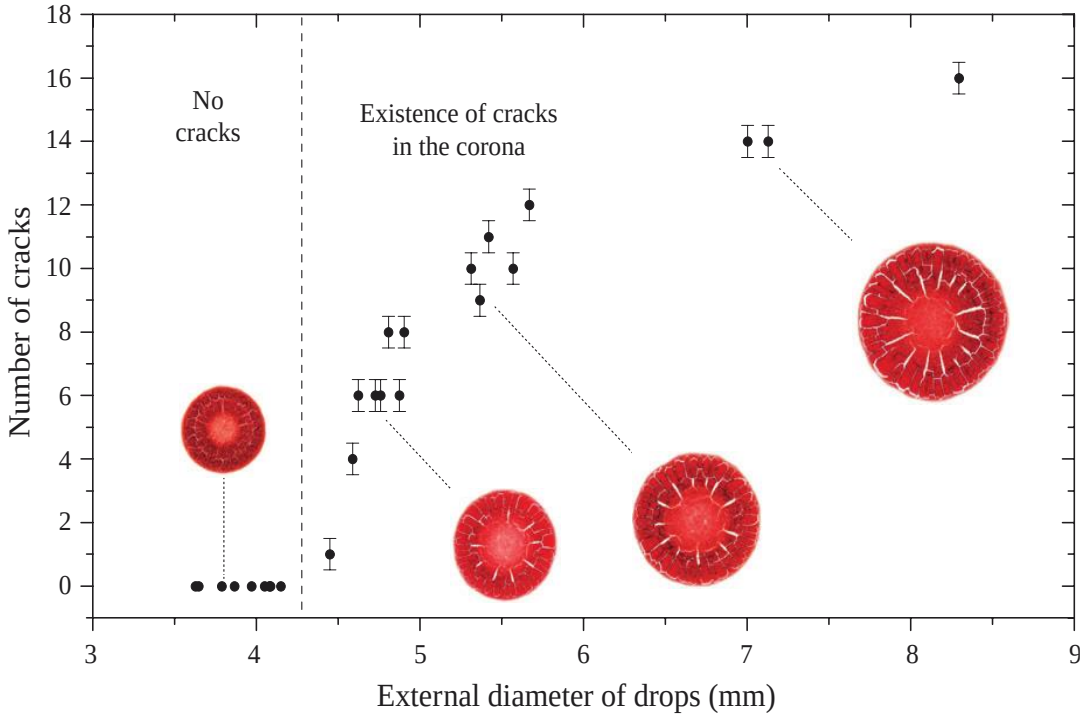

Figure 14.6

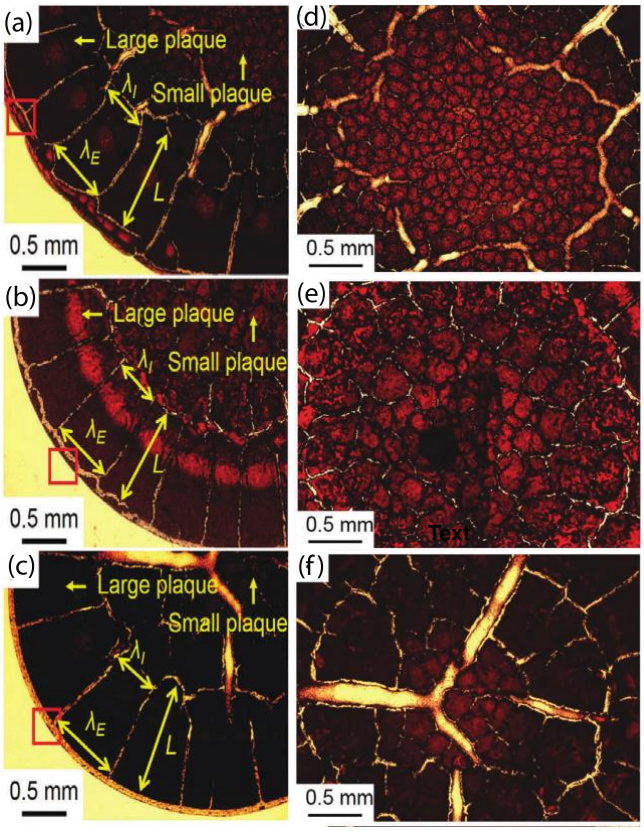

Figure 14.7

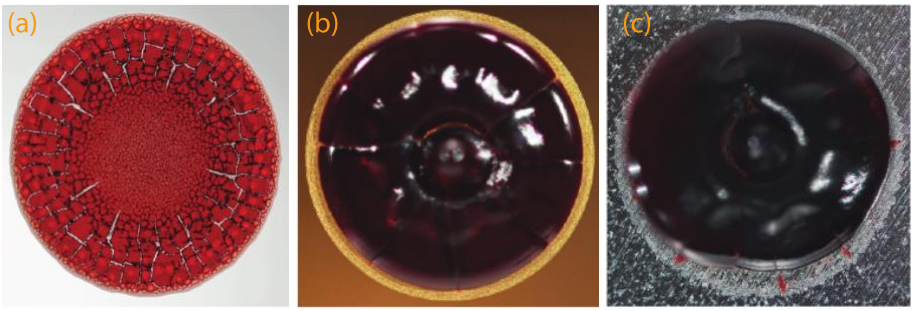

Figure 14.8

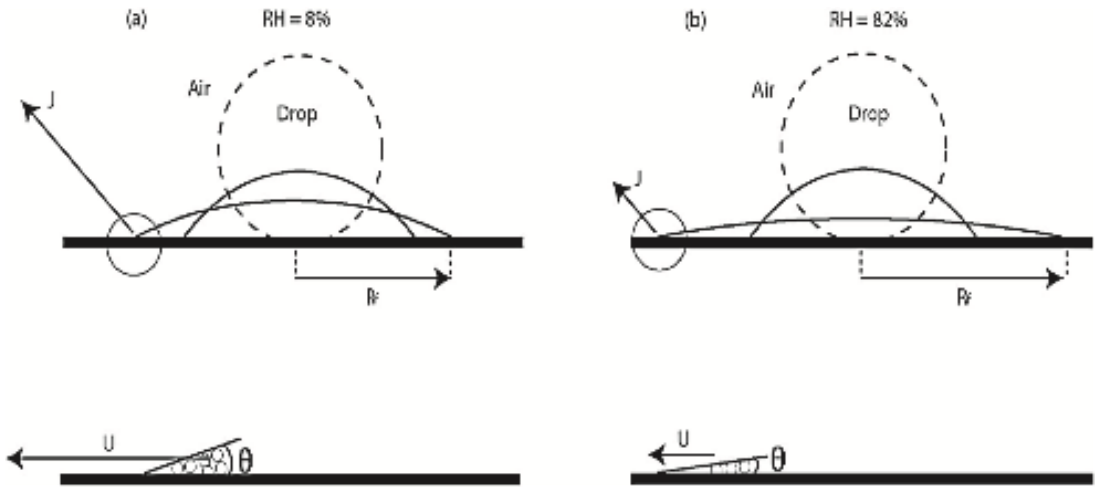

Figure 14.9

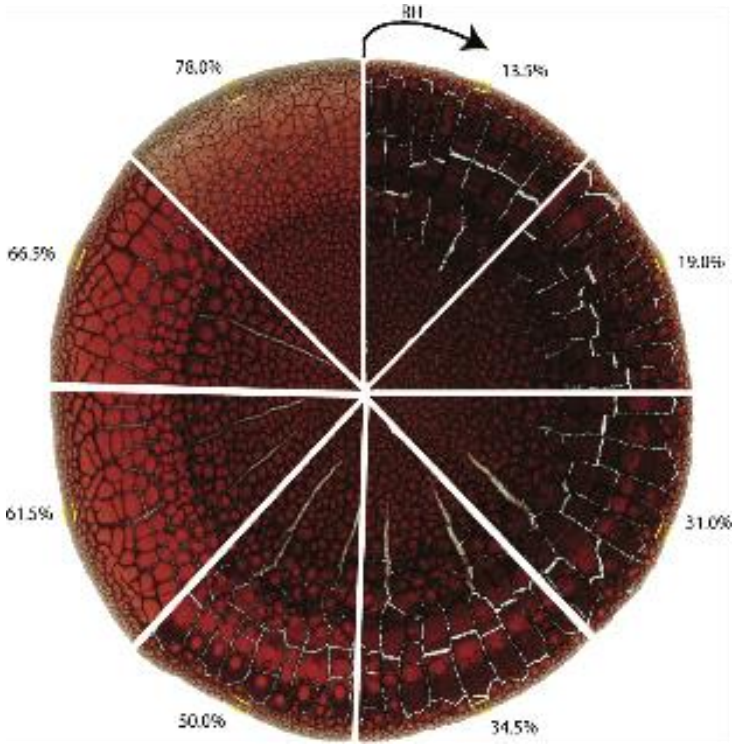

Figure 14.10

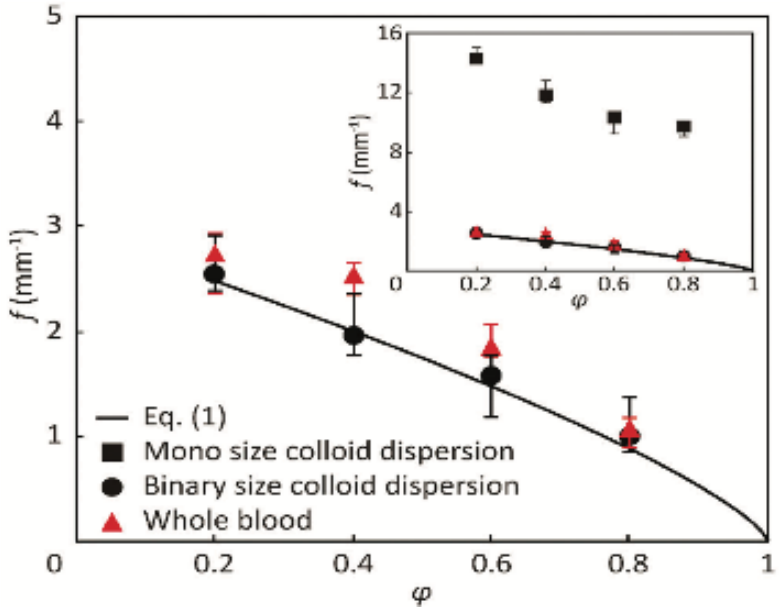
f (mm⁻¹)
φ
Eq. (1)
Mono size colloid dispersion
Binary size colloid dispersion
Whole blood

Figure 14.11

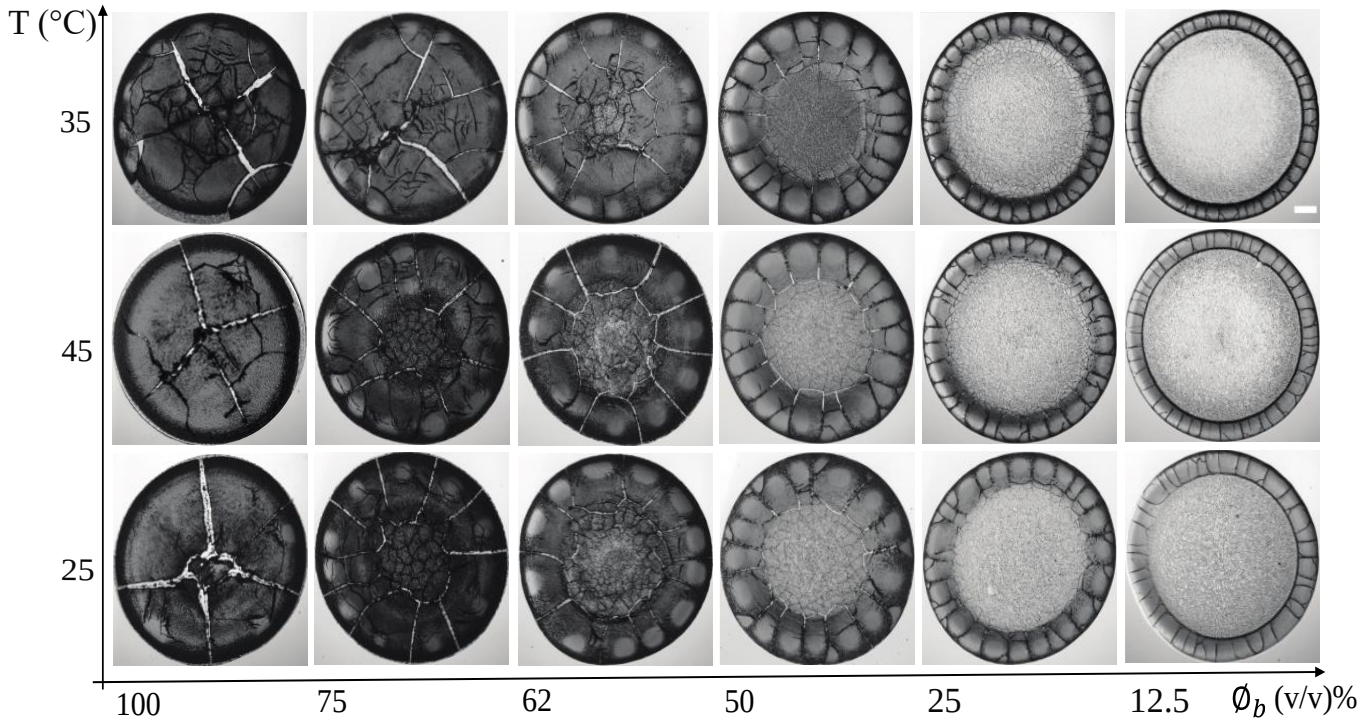
T (°C)
35
45
25
100
75
62
50
25
12.5
Ø_b (v/v)%